AFRL-RX-WP-TR-2013-0209

COLLABORATIVE RESEARCH AND DEVELOPMENT (CR&D) III

Task Order 0089: Dislocation Evolution and Crystal Plasticity Methods

Craig S. Hartley
El Arroyo Enterprises, LLC

NOVEMBER 2012
Final Report

AIR FORCE RESEARCH LABORATORY
MATERIALS AND MANUFACTURING DIRECTORATE
WRIGHT-PATTERSON AIR FORCE BASE, OH 45433-7750
AIR FORCE MATERIEL COMMAND
UNITED STATES AIR FORCE

NOTICE AND SIGNATURE PAGE

Using Government drawings, specifications, or other data included in this document for any purpose other than Government procurement does not in any way obligate the U.S. Government. The fact that the Government formulated or supplied the drawings, specifications, or other data does not license the holder or any other person or corporation; or convey any rights or permission to manufacture, use, or sell any patented invention that may relate to them.

This report was cleared for public release by the 88th ABW Public Affairs Office (Case Number: 88ABW-2013-4550, dated Oct 31, 2013) and is releasable to the National Technical Information Service (NTIS). It is available to the general public.

Qualified requestors may obtain copies of this report from the Defense Technical Information Center (DTIC) (http://www.dtic.mil).

AFRL-RX-WP-TR-2013-0209 HAS BEEN REVIEWED AND IS APPROVED FOR PUBLICATION IN ACCORDANCE WITH ASSIGNED DISTRIBUTION STATEMENT.

//SIGNATURE//
CHRISTOPHER WOODWARD, Project Engineer
Metals Branch
Structural Materials Division

//SIGNATURE//
DANIEL EVANS, Chief
Metals Branch
Structural Materials Division

//SIGNATURE//
ROBERT T. MARSHALL, Deputy Chief
Structural Materials Division
Materials and Manufacturing Directorate

This report is published in the interest of scientific and technical information exchange, and its publication does not constitute the Government's approval or disapproval of its ideas or findings.

REPORT DOCUMENTATION PAGE

Form Approved
OMB No. 0704-0188

1. REPORT DATE *(DD-MM-YY)*	2. REPORT TYPE	3. DATES COVERED *(From - To)*
November 2012	Final	30 April 2010 – 07 October 2012

4. TITLE AND SUBTITLE
COLLABORATIVE RESEARCH AND DEVELOPMENT (CR&D) III
Task Order 0089: Dislocation Evolution and Crystal Plasticity Methods

5a. CONTRACT NUMBER
FA8650-07-D-5800-0089

5b. GRANT NUMBER

5c. PROGRAM ELEMENT NUMBER
62102F

6. AUTHOR(S)
Craig Hartley

5d. PROJECT NUMBER
4347

5e. TASK NUMBER

5f. WORK UNIT NUMBER
X0R9

7. PERFORMING ORGANIZATION NAME(S) AND ADDRESS(ES)

El Arroyo Enterprises, LLC for: Universal Technology Corporation
231 Arroyo Sienna Drive 1270 N. Fairfield Road
Sedona, AZ 86336-6341 Dayton, OH 45432-2600

8. PERFORMING ORGANIZATION REPORT NUMBER

9. SPONSORING/MONITORING AGENCY NAME(S) AND ADDRESS(ES)
Air Force Research Laboratory
Materials and Manufacturing Directorate
Wright-Patterson Air Force Base, OH 45433-7750
Air Force Materiel Command
United States Air Force

10. SPONSORING/MONITORING AGENCY ACRONYM(S)
AFRL/RXCM

11. SPONSORING/MONITORING AGENCY REPORT NUMBER(S)
AFRL-RX-WP-TR-2013-0209

12. DISTRIBUTION/AVAILABILITY STATEMENT
Approved for public release; distribution unlimited.

13. SUPPLEMENTARY NOTES
PA Case Number: 88ABW-2013-4550; Clearance Date: 31 Oct 2013. This document contains color.

14. ABSTRACT (*Maximum 200 words*)
This research in support of the Air Force Research Laboratory Materials and Manufacturing Directorate was conducted for Wright-Patterson AFB, Ohio from 30 April 2010 through 07 October 2012. The objective of this research effort was to develop self-consistent methods for coarse graining results of dislocation dynamics simulations to inform crystal plasticity methods.

15. SUBJECT TERMS
dislocation dynamics, dislocation density vectors, micro-constitutive equations

16. SECURITY CLASSIFICATION OF:			17. LIMITATION OF ABSTRACT:	18. NUMBER OF PAGES	19a. NAME OF RESPONSIBLE PERSON (Monitor)
a. REPORT	b. ABSTRACT	c. THIS PAGE			Christopher Woodward
Unclassified	Unclassified	Unclassified	SAR	36	19b. TELEPHONE NUMBER *(Include Area Code)* (937) 255-9816

TABLE OF CONTENTS

Section **Page**

LIST OF FIGURES

Figure **Page**

1.0 SUMMARY

The research described in this report was initiated under Subcontract 10-S587-0089-01-C1, having the following SOW:

The contractor shall:

- Assist in creating a computer-driven research tool for the stereological analysis of the dislocation arrays produced by dislocation dynamic simulations, as provided by the on-site research staff.
- Employ the dislocation density description for glide and forest dislocations in order to establish the method as a reliable post processing tool for dislocation dynamics.
- Develop and validate micro-scale empirical constitutive-relationships relating dislocation content, distribution and evolution to local deformation (i.e. visco-plastic flow).
- Incorporate this description of dislocation density evolution into crystal plasticity methods, such as the Visco-Plastic Self Consistent crystal plasticity method, and validate this methodology.

Work performed was based on El Arroyo Enterprises Proposal dated April 9, 2010, which proposed a period of performance of May 1, 2010 through September 30, 2012. Consulting time for research was proposed at the rate of \$80.00/hr for 312 hrs. in each of FY 2010 and 2011 and 388 hrs. in FY 2012. Actual billing was for 161 hours in FY 2010, 367 hours in FY 2011 and 297 hours in FY 2012. Billing and monthly reporting were suspended after May 31, 2012 upon notification that the balance of funds originally authorized for FY 2012 was not available. As a result, only the first three items in the SOW were addressed during the period of performance.

The original quote from El Arroyo Enterprises also included line items for travel to W-PAFB approximately one time per fiscal year to discuss research progress with AFRL/RX personnel, and for publication costs for up to four articles in technical journals during the period of the agreement. As the work progressed, El Arroyo Enterprises elected to eschew billing separately for travel and publication expenses; to subsume the allocated funds into consulting hours and to absorb such expenses as might be incurred for these purposes from El Arroyo corporate resources.

In addition the Principal Investigator, Dr. Craig S. Hartley, was a guest researcher at the Max Planck Institut für Eisenforschung, Düsseldorf, Germany, during the periods May 1 - July 25, 2010 and June 6 - July 29, 2011, where he worked with MPIE personnel on development of the theory on which work on this subcontract is based. No consulting time was billed for this supporting effort.

Results of research related to the subject of this subcontract were presented at six international scientific meetings, listed below.

1. “Representation of Dislocation Dynamics Simulations", Craig S. Hartley, Jaafar A. El Awady and Christopher Woodward, Proceedings of MMM 2010, October 4 - 8, 2010, Freiburg, Germany

2. "Mobility of Dislocation Populations as a Thermally Activated Process", Craig S. Hartley, TMS Annual Meeting, 2011, San Diego, CA
3. "Dislocation Evolution During Plane Bending of a BCC Crystal", Craig S. Hartley, Bing Liu and Dierk Raabe, Proceedings of Plasticity 2012, San Juan, PR
4. "Direct and Derived Dislocation Density Vectors", Craig S. Hartley, TMS Annual Meeting 2012, Orlando, FL
5. "Multiscale Modeling - Extending the Design Space" Mechanics of Materials, Mathematisches Forschungsinstitut Oberwolfach, March 18 - 24, 2012, Oberwolfach, Germany
6. "Dislocation Density Vectors in FCC Crystals Deformed in Plane Strain", Craig S. Hartley, to be presented at Plasticity 2013, Nassau, Bahamas, Jan. 3 – 9, 2013.

In addition to these presentations two scientific papers have been prepared and submitted based on the research supported by this subcontract. The first, a paper co-authored by Craig S. Hartley, J. A. El Awady, B. Liu, C. Woodward and D. Raabe, was submitted first to Acta Materialia in 2010 and rejected as not appropriate for the journal. The paper was revised and submitted to Modeling and Simulation in Materials Science and Engineering later in 2011. This journal required revision of the manuscript before reconsideration for publication. Dr. Hartley has now taken the responsibility for revising the manuscript based on referee's comments, later results and developments and preparing it for submission to MSMSE or another scientific journal.

Dr. Hartley co-authored a paper with Dr. J. A. Clayton and Prof. D. McDowell on the topic of the physical interpretation of terms involved in the decomposition of total deformation. This work forms the foundation of the interpretation of the components of deformation that make up the description of the dislocated crystal. In this paper we point out that conventional interpretation of the components of deformation employed in contemporary treatments of crystal plasticity fail to account for the lattice deformation due to internal defects, which is the source of internal stresses. A modification to the conventional means of expressing the decomposition is proposed, which accounts for this missing term. The paper has been submitted to the International Journal of Plasticity, where it will appear in a special issue commemorating the contributions of Prof. Hussein Zbib.

The first section of this report summarizes the principal features of the modifications to the mathematical treatment of continuum mechanics and crystal plasticity introduced by consideration of the additional component of distortion due to dislocations and internal defects. Next, we review important features of the Dislocation Density Vector concept. Next, we introduce the concept of the Direct and Derived DDVs that put into vector form the concepts of Geometrically Necessary and Statistically Stored dislocation content introduced by Ashby [2]. Following that, we describe the application of this concept to the description of results of Dislocation Dynamics calculations and selected experiments. Recommendations based on the results of this research conclude the report.

2.0 INTRODUCTION

The critical interface between physics-based models of deformation and the design process occurs when models of deformation at the microscopic scale are inserted into codes employed to design engineering components at the macroscopic scale. This involves creating a transition from the physicists' view of deformation of crystals as a many-body problem governed by the laws of atomic physics to the mechanist/designer's point of view that regards engineering materials as continua with properties determined by empirical methods. In the former case the fundamental entities are atoms or groups of atoms, while the latter considers structures on a scale determined by the size of the application. The task of applying knowledge of material properties and behavior at the atomic scale to inform models employed in engineering design has proved to be one of the most enduring challenges of modern engineering science.

Research performed on this subcontract was initiated to exploit advances in computational models of the behavior of groups of dislocations, known as Dislocation Dynamics (DD), to develop analytic expressions relating the behavior of such groups to the external forces required to change the shape of crystals of finite size and a quantitative description of the resulting deformation. Such expressions, called micro-constitutive equations (MCE), are necessary input to models of material behavior employed in engineering design codes.

The process begins by constructing a computational volume with properties characteristic of a selected material. Within this volume, dislocation sources are initially present, having distortion fields calculated from well-established equations of dislocation mechanics. At a series of computational steps, the test volume is subjected to known boundary conditions, causing the initial dislocation configuration to respond to these as well as to the mutual forces between dislocations. The output of the calculations at each step consists of a listing of the instantaneous positions of the dislocation segments as well as any new dislocations resulting from possible interactions among prior existing dislocations. This output is typically displayed in a visual format, often as an animated sequence of successive dislocation structures. At present there is no universally accepted means of describing quantitatively the ensemble of dislocations in the deformed structure in a form that would be useful to employ in the construction of MCEs.

An attractive feature of the computational DD approach lies in the fact that it can be applied to perform virtual experiments at a physical scale generally incapable of being achieved by comparable experiments on real crystals. In the few cases where such physical experiments have been performed, they have been shown to be difficult to interpret and to apply to the deformation of crystals at the larger scales required for most engineering components [33, 34]. Therefore a compelling argument exists for employing computational methods, such as DD, to supplement experiments on real materials by performing selected calculations in order to create a broader, physics-based modeling process for describing the behavior of engineering materials [26]. The principal challenge lies in the development of suitable means of employing the results of such calculations in the construction of the relationships necessary for use in engineering design codes. The research described in this report addresses several aspects of this problem.

3.0 METHODS, ASSUMPTIONS, AND PROCEDURES

3.1 Review

Analysis of deformation of a crystalline body is typically based on approximating the atomic array by a continuum, throughout which source and response fields are continuously distributed. When crystal defects are present these fields are not necessarily continuous and continuously differentiable, but can contain a finite population of discontinuities. The success of approximating a many-body treatment by a continuum field theory relies on the applicability of the ergodic assumption that the ensemble averages of properties of the discrete array are adequately approximated by the temporal and volumetric averages of the properties taken over the volume occupied by the array and the time of observation.

It follows that there exists a regime of size[*] where ensemble averages can replace continuum variables in the application of field theories of deformation. This approximation of an array of discrete atoms by a continuous distribution of matter is adequate for treating deformation of material volumes containing a large population of atoms and defects in the atomic array. In the following discussion we employ this concept to define such quantities as the deformation gradient and the incompatibility associated with deformation of a continuum.

Approximations made to obtain solutions for deformation problems in crystalline materials containing dislocations frequently obscure the local character of the dislocation distribution. Such approximations are usually justified on the basis of the scale of the problem being solved, e.g. if only far-field properties are of interest, the details of a dislocation distribution with a zero resultant Burgers vector may be ignored. However when stresses, strains and lattice rotations at the level of the mean spacing between dislocations are of interest, the details of the distribution become a major part of the problem being solved.

The dislocated continuum introduced by Kröner [17, 18, 19], widely employed in the literature on crystal plasticity [8, 28] is built up of a mosaic of compact elements having slightly different lattice orientations. In this "mosaic continuum" deformation of the elements occurs by the passage of dislocations entirely through them, so that when the elements are joined together to form the global body, the dislocations reside entirely at the interfaces between the elements. Thus the incompatibility that characterizes the misfit between elements is localized on these interfaces. In the limit as the average size of the elements approaches zero, the distribution of surface dislocations approaches a continuous distribution of dislocations in the body and the incompatibility becomes global.

In structures with microstructure of a finite size the mosaic continuum ignores the contribution of dislocations within the blocks. This neglect is justified by assuming that the addition of a "homogeneous" distribution of dislocations, i.e. one in which the net Burgers vector vanishes, has an inconsequential effect on the deformation process. While this assumption may suffice for large-scale deformation problems, such as those occurring in metal forming calculations; [32], it can only be strictly true if the reference state is a "natural" state [17, 31] in which the homogeneous distribution of dislocations is initially present and takes no part in any subsequent deformation.

---

[*] For the remainder of this treatment we ignore the temporal aspect of the approximation and concentrate on the spatial.

Also, the contribution of gradients in lattice strain to the mechanical behavior of crystals requires analyses on the scale of the mean spacing of dislocations [8]. Finally, investigations of the evolution of dislocation structures and their contribution to the global deformation and stress fields require a clear understanding of how descriptions of a dislocation population at different levels of resolution relate to one another and to the physical nature of the dislocation arrangement. In the following section we review the description of deformation using concepts of continuum mechanics and lattice geometry to illustrate that current usage of continuum deformation fields in crystal plasticity needs modification in order to account fully for the effects of dislocations.

In order to have a concise reference to the definition of the deformation gradient concept in continuum mechanics, the development in this section follows the excellent summary of this topic due to Gullett et al. [10]. Consider a continuous body composed of an assembly of material points whose locations are specified by position vectors in the initial configuration. The operation

$$\mathbf{x} = \chi(\mathbf{X}) \tag{1}$$

maps a point at **X** in the reference configuration, Ω_0, to its image at **x** in the current, or deformed, configuration, Ω. The deformation gradient, F, defined as

$$\mathbf{F} = \frac{\partial \chi}{\partial \mathbf{X}} = \frac{\partial \mathbf{x}}{\partial \mathbf{X}} \tag{2}$$

specifies the local deformation at **X**.

$$d\mathbf{x} = \chi(\mathbf{X} + d\mathbf{X}) - \chi(\mathbf{X}) \tag{3}$$

which, when expanded to first order in d**X**, yields

$$d\mathbf{x} \approx \nabla\chi(\mathbf{X})d\mathbf{X} = \mathbf{F}d\mathbf{X} \tag{4}$$

by the definition of F, Equation (2). The existence of a continuous displacement vector field, u:

$$\mathbf{u} = \mathbf{x} - \mathbf{X} \tag{5}$$

whence

$$\mathbf{F} = \mathbf{I} + \frac{\partial \mathbf{u}}{\partial \mathbf{X}} \tag{6}$$

insures the existence of a one-to-one mapping from the reference to the deformed state and the integrability of F throughout the medium. The integrability condition can be expressed in terms of the incompatibility, η, a symmetric, second-rank tensor defined as [19].

$$\boldsymbol{\eta} = \nabla \times \mathbf{F} \times \nabla \tag{7}$$

which vanishes identically if u is continuous and thrice differentiable. Application of the definition in Equation (7) requires that F have derivatives up to the second order at the point X.

Finally we observe that the deformation of a body relative to the reference configuration can be described by computing the change in squared length of the reference vector:

$$\mathbf{dx}^{\mathrm{T}}\mathbf{dx} - \mathbf{dX}^{\mathrm{T}}\mathbf{dX} = \mathbf{dX}^{\mathrm{T}}(\mathbf{C} - \mathbf{I})\mathbf{dX} \tag{8}$$

where the superscript T indicates the transpose of a matrix and $\mathbf{C} = \mathbf{F}^{\mathrm{T}}\mathbf{F}$ is the right Cauchy-Green tensor. Measures of strain referred to the reference and current states are defined in terms of the dimensionless, symmetric, second order tensor in parentheses.

We note that as a consequence of the first order approximation, Equation (6), the magnitude of the stretch ratio, $\lambda = |d\mathbf{x}|/|d\mathbf{X}|$, is a function of $\mathbf{t} = d\mathbf{X}/|d\mathbf{X}|$, the unit vector in the direction of $d\mathbf{X}$:

$$\lambda^2 = \frac{|\mathbf{dx}|^2}{|\mathbf{dX}|^2} = \mathbf{t}^{\mathrm{T}}(\mathbf{C})\mathbf{t} \tag{9}$$

which is the equation for an ellipsoid in the reference state having a radius $1\backslash\lambda$ measured from P in the direction of $\mathbf{t}$. The angle, $\theta(\mathbf{t})$, between $d\mathbf{X}$ and its image in the deformed state, $d\mathbf{x}$ can be determined from

$$\theta(\mathbf{t}) = \cos^{-1}\left[\frac{\mathbf{dx}^{\mathrm{T}}\mathbf{dX}}{|\mathbf{dx}||\mathbf{dX}|}\right] = \cos^{-1}\left(\frac{\mathbf{t}^{\mathrm{T}}\mathbf{F}^{\mathrm{T}}\mathbf{t}}{\lambda}\right) \tag{10}$$

The unit vector $\mathbf{t}$ in the reference state becomes the unit vector $\mathbf{t}' = d\mathbf{x}/|d\mathbf{x}|$ in the deformed state, where the vectors are related by

$$\mathbf{t}' = \frac{\mathbf{Ft}}{\lambda} \tag{11}$$

In the next section these equations will be used as the basis of a method for determining an effective value for F in cases where the absence of a continuous displacement field precludes determination of the deformation gradient by direct differentiation, i.e. the incompatibility does not vanish.

3.2 Deformation Gradient in the Dislocated Discrete Lattice

We now consider examples where the lack of a single-valued, continuous displacement vector renders Equation (6) inappropriate as a definition for F, i.e. when Equation (5) does not result in a single-valued, continuous and continuously differentiable displacement field. Initial positions are known for all atoms in the array from the choice of a reference structure, usually a perfect single crystal. After introducing a defect that maintains the material continuity, but not necessarily the local crystal symmetry throughout, the final configuration is determined by minimizing the internal energy of the array or some similar criterion. Thus, the atomic positions are known in the "deformed" configuration to the same degree of precision as for the reference configuration. For most of the region it is possible to identify the initial and final positions of individual atoms. However in the presence of a defect that disrupts the local crystal symmetry, such identification may not be possible. The question at issue is: how are descriptions of these discrete systems related to the continuum model described in the previous section?

The following development follows that of Bilby et al. [4], but where possible employs notation consistent with the continuum mechanics notation of the previous section. The lattice deformation is obtained by choosing three non-coplanar basis vectors directed along the same local principal crystallographic directions in each state at every atomic location in the reference and dislocated (deformed) crystal. A basis vector in these triads is indicated by $i\alpha$, $\alpha = 1\ldots3$, for

the perfect lattice and the corresponding vector by ek, k = 1… 3, for the dislocated lattice. At a typical lattice point, P, these vectors are related by a local deformation, Fkα, defined by

$$\mathbf{e}_k = \mathbf{F}_{k\alpha}(\mathrm{P})\mathbf{i}_\alpha \tag{12}$$

where the argument, P, emphasizes that the deformation matrix applies to the point, P and we have dispensed with the contra- covariant notation employed by Bilby *et al*. We also assume that the deformation has an inverse such that

$$\mathbf{i}_\beta = \mathbf{F}^{-1}_{\beta j}(\mathrm{P})\mathbf{e}_j \tag{13}$$

A position vector, **X**, in the reference state is $\mathbf{X} = X_\alpha \mathbf{i}_\alpha$ and in the deformed state, $\mathbf{x} = x_k \mathbf{e}_k$. Equations (12) and (13) perform the same function relating vectors in a perfect reference lattice to their counterparts in the deformed lattice as does Equation (6) (and its inverse) for a continuum. However, Equations (12) and (13) are constrained by considerations of local crystal symmetry whereas Equation (6) is not. Also Equations (12) and (13) apply to a finite number of atoms located at specific positions in the vicinity of P rather than an arbitrary set of mathematical points. The deformation measured as described above is necessarily a lattice deformation, since all measurements are made directly on atomic positions in the array. For computational convenience, both sets of basis vectors are generally expressed in terms of their components relative to a "laboratory" (L) Cartesian coordinate system having basis vectors, **y**, using the transformations $L_{i\alpha} = \mathbf{y}_i \cdot \mathbf{i}_\alpha$ and $L'_{km} = \mathbf{y}_k \cdot \mathbf{e}_m$.

While it is possible in principle to determine the deformation matrix by using the positions of atoms in the perfect reference lattice and in the deformed lattice to solve Equation (12) or (13) directly, this can only be done unambiguously in the absence of crystal defects. When defects, such as dislocations, are present the identification of atoms in the deformed state with their positions in the reference state is not unambiguous. See, for example, the discussion of Hartley and Mishin [15] on this point. A lattice correspondence matrix, $\mathbf{F}_{\square\square}(\mathrm{P})$, is defined for each neighbor to the atom at P in terms of the lattice vectors connecting these atoms for a selected number of near neighbor shells:

$$\mathbf{x}_{(\square')}(\mathrm{P}) = \mathbf{F}_{(\square\square)}(\mathrm{P})\mathbf{X}_{(\square)}(\mathrm{P}) \tag{14}$$

The number of shells can be formally as large as desired[†], but for single point and line defects in crystals, the range of the interatomic forces between atoms determines the number.

In studies of dislocations in bcc and fcc crystals, Hartley and Mishin [15] chose atoms lying within a sphere of radius $R = (R_1 + R_2)/2$, where R_1 and R_2 are, respectively, the first and second neighbor coordination radii in the perfect lattice[‡]. Since the structural ambiguity introduced by the presence of a defect in the computational cell renders it impossible to obtain a single matrix that will satisfy Equation (14) for all pairs of neighbors, it is necessary to employ a procedure that yields a "best fit", in the least-squares sense, to $\mathbf{F}_{\delta'\delta}(\mathrm{P})$ as applied to a selected set of neighboring atoms [10, 15] in order to obtain an analogue to the continuum definition of **F**.

[†] The number of shells considered is a measure of the "graininess" of the approximation.
[‡] This sphere is henceforth called the calculation volume.

Designate by $[\mathbf{X}(P)]^{(\delta)}$, $\delta = 1 \ldots N$, the set of vectors connecting the N atoms neighboring P within the calculation volume in the perfect lattice. Let $[\mathbf{x}(P)]^{(\delta')}$, $\delta' = 1 \ldots N'$, be the corresponding set in the deformed lattice. With no defect in the computational volume, the same neighbors are unambiguously identified before and after deformation, $N = N'$ and $\delta = \delta'$. However when a defect is exists, some ambiguity of choice is often present. Identification of neighbors may have to be based on criteria that preserve local lattice symmetry [15] or some similar considerations, and may, in fact, not be unique. Having selected N' pairs of vectors $[\mathbf{X}(P)]^{(\delta')}$ and their images $[\mathbf{x}(P)]^{(\delta')}$ we now have N' equations of the form of Equation (14). The set of 3N equations relating $[\mathbf{X}(P)]$ to $[\mathbf{x}(P)]$ for each set of measurements can be written

$$\widehat{\mathbf{x}} = \hat{\mathbf{F}}\widehat{\mathbf{X}} \tag{15}$$

where $\widehat{\mathbf{X}}$ and $\widehat{\mathbf{x}}$ are each 3 x N' matrices whose columns are the components of the vectors $[\mathbf{X}(P)]^{(\delta')}$ and $[\mathbf{x}(P)]^{(\delta')}$, respectively, and $\hat{\mathbf{F}}$ is a 3 x 3 matrix that minimizes the squares of all the residuals between the measured vectors and vectors calculated using $\hat{\mathbf{F}}$. The least-squares solution to Equation (15) has the form

$$\hat{\mathbf{F}} = \widehat{\mathbf{x}}\underset{\sim}{\mathbf{X}} \tag{16}$$

where

$$\underset{\sim}{\mathbf{X}} = \left(\widehat{\mathbf{X}}^{\mathrm{T}}\widehat{\mathbf{X}}\right)^{-1}\widehat{\mathbf{X}}^{\mathrm{T}} \tag{17}$$

is generalized inverse, or Moore-Penrose matrix, for $\widehat{\mathbf{X}}$. The matrix of coefficients that compose $\hat{\mathbf{F}}$ is the analogue to the deformation gradient at P in a discrete lattice.

In analyzing the local continuity of **F** in the vicinity of a dislocation, it is necessary to obtain an expression for its curl at points, P, in the neighborhood. Hartley and Mishin accomplished this by combining finite differences of appropriate components of **F** evaluated at P and its nearest neighbors (in the perfect reference lattice). The accuracy of such a calculation depends, naturally, on the size of the computational volume, but satisfactory results were obtained for cells of the size employed by Hartley and Mishin.

3.3 The Description of Deformation and the Mechanical Cycle

We[§] begin by noting with Bilby, Gardner, & Smith [5] that:

> *In describing the deformation of a crystal containing dislocations it is essential to distinguish between the deformation of the crystal lattice and that of a three-dimensional grid affixed to the body and deforming congruently on the micro-scale with the overall shape change of the crystal.*

In fact, trying to analyze the deformation of a crystal lattice in terms "a three-dimensional grid affixed to the body and deforming congruently on the micro-scale with the overall shape change of the crystal" is analogous to trying to describe the positions of oranges in a bag by analyzing the change of shape of the bag.

[§] The treatment in this section is adapted from a paper written in collaboration with Dr. J. A. Clayton and Prof. D.L. McDowell and contains elements of their review and input.

The following development adapts the notation introduced by Bilby, Bullough and Smith [4] for describing the components of crystal deformation referred to basis vectors associated with deformation of the lattice and relating this basis set to one associated with changes of the overall shape change of the body. Our adaptation consists of noting that the lattice correspondence functions introduced by Bilby *et al.*, which relate the lattice and shape coordinate systems, correspond to certain components of the deformation gradient employed in continuum plasticity. This differs from the notation employed in much of the mechanics literature, [17, 22], which does not distinguish between lattice and spatial coordinates. We choose the former because of its emphasis on the physical origins of the coordinate bases.

Kröner [17] explicitly recognized the dual nature of the deformation by noting that the deformed crystal is a Cosserat continuum in which each mathematical point is associated with two sets of directors. Coordinate systems required to describe deformation of the crystalline body are: 1) spatial coordinates, or shape coordinates, which have basis vectors at each material point that are parallel to coordinate axes in a system that describes the instantaneous geometric shape of the body without reference to the underlying atomic structure, and 2) material coordinates, or lattice coordinates, which have basis vectors parallel to the local principal crystallographic directions. These basis vectors are the directors in a modified Cosserat continuum used to model the material.

Basis vectors in the crystal lattice connect lattice points, while those in the shape coordinates connect material points, which are, in general, a collection of lattice points that occupy a region called a Representative Volume Element (RVE) [28] or a Statistical Volume Element (SVE) [24]. In this view the element becomes the material "point", which is understood to be a region of the crystal that contains a collection of lattice points. The coordinates of the material points are located at the centroids of these volume elements, which form the nodes of the shape coordinate system, while lattice points form the corresponding set in the lattice coordinates.

While the manifolds of material points and lattice points occupy the same physical region in space, they are not coincident. Depending on the dislocated state within a RVE there may or may not be an affine connection between shape coordinates and lattice coordinates. Finally we note that applying crystal plasticity concepts to polycrystalline materials may require associating several hundred grains of differing orientations to a single material point [3]. In the following discussion we restrict our consideration to a single crystal containing dislocations, for which material points consist of groups of neighboring atoms within the crystal.

We now consider the deformation of a local RVE of defect-free crystalline material bounded by a surface Σ and removed from the bulk crystal. Each such element initially fits exactly into its neighborhood such that the global reference configuration is simply connected. This reference state is unique, in contrast to a "natural state" [17, 31] which can contain an arbitrary distribution of internal defects that produce a self-equilibrating field of internal stress.

We call the "mechanical cycle" a hypothetical mechanical process that converts the RVE from the reference state to the current (deformed) state in a manner analogous to that in which the Carnot cycle, a thermodynamic process, converts heat to work. For the present we consider only conservative deformation processes, so that lattice sites in the element are conserved. During the mechanical cycle the RVE adopts the following local configurations, or states:

- B_0 is the initial *reference state*, in which the RVE contains an unstressed perfect lattice, bounded by a traction-free surface, Σ, at some initial time, t_0.

- $\tilde{\mathbf{B}}$ is the *stress-free intermediate state*, formed from B_0 at constant internal energy, where the RVE also contains an unstressed slipped lattice with traction-free Σ.
- $\bar{\mathbf{B}}$ is the *internally stressed intermediate state*, formed from $\tilde{\mathbf{B}}$ at constant configurational entropy, where the RVE contains a slipped lattice with internal stresses and a traction-free Σ.
- B is the *current state*, formed from the appropriate intermediate state by applying suitable tractions on Σ, consisting of an externally and internally stressed slipped lattice at some time, t.

The reference configuration B_0, describes the RVE embedded within a larger slab of homogeneous material that is also unstressed in its (global) reference configuration. This is always a compact state in which shape and lattice coordinates are related by an affine transformation. The local current configuration B of the element is achieved when the element is stressed and deformed, along with its neighbors, so that all volume elements fit together and the body is simply connected in the global current configuration.

Deformation of the RVE from B_0 to B occurs by passing through intermediate configurations as noted above. There may be one or two such configurations, depending on the nature of dislocation motion. The compact and non-compact forms of the intermediate configuration $\tilde{\mathbf{B}}$, are formed in the following manner:

1) The compact form results when all dislocations pass entirely through the element, in which case $\tilde{\mathbf{B}}$ is a compatible state. Work done by external stresses is converted to heat and an increase in surface energy due to the formation of additional external surface area at slip steps on Σ where dislocations have entered and/or exited the element.

2) The non-compact form results when some dislocations pass only part-way through the element, so that the lattice remains stress-free by introducing atomic-scale Mode I cracks across whose surfaces the atoms are not in contact. Work done by external stresses is converted to heat and surface energy, as in 1).

In case 1, re-insertion of the element into the matrix replicates the process employed by Kröner [17] to form an element of the “mosaic” continuum and is also the basis of Eshelby's treatment of the elastic inclusion [7].

If $\tilde{\mathbf{B}}$ is not a compact state, we require the element to pass through a second local intermediate configuration, $\bar{\mathbf{B}}$, that is compact, prior to re-insertion into the slab. This configuration is formed by collapsing the lattice around the internal discontinuities left by partial traverses of dislocations across the element in $\tilde{\mathbf{B}}$, thus restoring the continuity of the lattice and forming lattice defects at these locations. Deformation from $\tilde{\mathbf{B}}$ to $\bar{\mathbf{B}}$ occurs at constant configurational entropy, since no dislocation motion occurs. However there will be a small increase in entropy due to changes in the lattice vibrational modes when the internal surfaces are removed by joining the adjacent crystal faces. The surface energy of these internal surfaces is converted, irreversibly, to strain energy, resulting in a state of self-stress. Surface steps on Σ created by the entrance and exit of dislocations from the element remain. Since the element is traction free on Σ, the resulting state of internal stress is self-equilibrating. When $\tilde{\mathbf{B}}$ is a compact state, all

dislocations have completely traversed the RVE and $\bar{\mathbf{B}} \Rightarrow \tilde{\mathbf{B}}$, *i.e.* there is only one, stress-free, intermediate state.

The current state is formed from a compact intermediate state at constant configurational entropy. It is accompanied by an increase in internal energy due to the reversible response of the crystal to the imposition of tractions on Σ by external forces and the stress fields of defects elsewhere in the body. The RVE may contain internal crystal defects plus surface dislocations created at the interface of Σ and the remainder of the crystal when the RVE is re-inserted in the bulk crystal.[**].

The *Shape Deformation*, $\mathbf{F}^S$, causes the element to change its configuration from B_0 to B. Since this deformation converts a compact state to a compact state, it is by definition compatible and can be written in terms of the gradient of a displacement vector, **u**,

$$\mathbf{F}^S = \mathbf{I} + \nabla\mathbf{u} \tag{18}$$

where **I** is the unit tensor and both the vector and the gradient are expressed in shape coordinates. The *Dislocation Deformation*, $\mathbf{F}^D$, is the volume average of the shape deformation of the RVE in passing from B to $\tilde{\mathbf{B}}$, expressed in shape coordinates. Since this deformation, by definition, does not deform the crystal lattice, it is a stress-free deformation. With M active slip systems on which dislocations of the k^{th} system sweep out an area, $A^{(k)}$, per unit volume

$$\mathbf{F}^D = \mathbf{I} + \sum_{k=1}^{M} \left[\mathbf{b}^{(k)} \otimes \mathbf{A}^{(k)} \right] \tag{19}$$

where $\mathbf{b}^{(k)}$ is the Burgers vector of the dislocations and $\mathbf{A}^{(k)}$ is a vector with magnitude $A^{(k)}$ that points in the direction of the positive normal to the k^{th} slip plane. The summation in Equation (19) is often written in terms of the shear strain associated with slip on the k^{th} system, $\gamma^{(k)}$, and the Schmid tensor, $\mathbf{S}^{(k)} = \eta^{(k)} \otimes \nu^{(k)}$, where η and ν are unit vectors along the slip direction and normal to the slip plane of the system, respectively. This is the source of the *eigenstrain* described by Kröner [19].

Since the lattice remains undeformed, the process occurs at constant internal energy. However it causes an increase in configurational entropy due to the fact that, depending on the size of the element and the availability of slip systems, there are, in general, several ways that dislocations can traverse the element and produce the same $\mathbf{F}^D$. In addition to this entropy increase, there is an increase in surface energy of the element due to the surfaces created by the slip steps produced on Σ at the entry and exit locations of dislocations and by internal discontinuities caused by dislocations that do not completely traverse the element.

Lattice distortion introduced by defects created by elimination of internal surfaces causes a change in internal strain energy as well as in the shape of the element in state $\bar{\mathbf{B}}$. This *Incompatible Lattice Deformation*, $\mathbf{F}^{LD}$, is the *lattice deformation field due to the dislocations now present within the element,* expressed in lattice coordinates. The components of $\mathbf{F}^{LD}$ correspond to the Lattice Correspondence Functions introduced by Bilby and co-workers [4] that

[**] Eshelby Eshelby, 1957) treats this misfit as a distribution of surface force, but notes that it can also be a distribution of dislocations.

connect lattice basis vectors to basis vectors in the shape coordinate system. This incompatible lattice deformation modifies $\mathbf{F}^D$ to give $\mathbf{F}^P$, the plastic deformation, which is a compatible, irreversible deformation associated with passage from B_0 to $\bar{\mathcal{B}}$: $\mathbf{F}^P = \mathbf{F}^{LD}\mathbf{F}^D$. We repeat for added emphasis that if $\mathbf{F}^D$ produces a compatible deformation due to dislocations passing entirely through the element, $\bar{\mathcal{B}} \Rightarrow \tilde{\mathcal{B}}$, $\mathbf{F}^{LD} = \mathbf{I}$ and $\mathbf{F}^P = \mathbf{F}^D$.

The volume element is deformed to the current state, B, by the application of appropriate tractions to Σ and re-insertion of the element into its original location in the slab. This operation carries the compact state $\bar{\mathcal{B}}$ to the compact state B, hence it is a compatible deformation. This is the *Compatible Lattice Deformation*, $\mathbf{F}^{LC}$. Note that it is the component generally called "elastic deformation" in treatments that ignore the presence of incompatible lattice distortion due to internal defects. The components of $\mathbf{F}^{LC}$ are also Lattice Correspondence Functions, connecting lattice to shape coordinates. Together the two lattice distortion components comprise the *Lattice Deformation*, $\mathbf{F}^L$, introduced by Bilby, *et al*. [4].

The necessity for separating the lattice deformation into components due to internal sources and external sources has been noted previously the present author [12] and others in various contexts [6, 9, 16, 23, 29]. The expression relating the components assumes that of the familiar multiplicative decomposition of total finite deformation:

$$\mathbf{F}^S = \left(\mathbf{F}^{LC}\mathbf{F}^{LD}\right)\mathbf{F}^D = \mathbf{F}^L\mathbf{F}^D \tag{20}$$

which introduces a third component of deformation due to the separation of the lattice deformation into compatible and incompatible components resulting from the presence of dislocations and other crystal defects.

Relationships of the deformation components to the various states of deformation are summarized below:

- $\mathbf{F}^S$: shape deformation associated with configuration change $B_0 \rightarrow B$
- $\mathbf{F}^D$: stress-free shape deformation due to dislocation motion all or part way through the element; associated with configuration change $B_0 \rightarrow \tilde{\mathcal{B}}$
- $\mathbf{F}^{LD}$: lattice deformation due to self-stress of dislocations inside the element; associated with configuration change $\tilde{\mathcal{B}} \rightarrow \bar{\mathcal{B}}$
- $\mathbf{F}^{LC}$: compatible lattice deformation due to traction applied to the RVE boundary; associated with configuration change $\bar{\mathcal{B}} \rightarrow \mathcal{B}$
- $\mathbf{F}^L = \mathbf{F}^{LC}\mathbf{F}^{LD}$: lattice deformation (Lattice Correspondence Functions) due to all sources; associated with configuration change $\tilde{\mathcal{B}} \rightarrow \mathcal{B}$
- $\mathbf{F}^P = \mathbf{F}^{LD}\mathbf{F}^D$: shape deformation remaining after release of external tractions on RVE; associated with configuration change $\mathcal{B}_0 \rightarrow \bar{\mathcal{B}}$. Same as $\mathbf{F}^D$ iff $\tilde{\mathcal{B}} = \bar{\mathcal{B}}$.

Configurations and deformation mappings are illustrated in Figure 1.

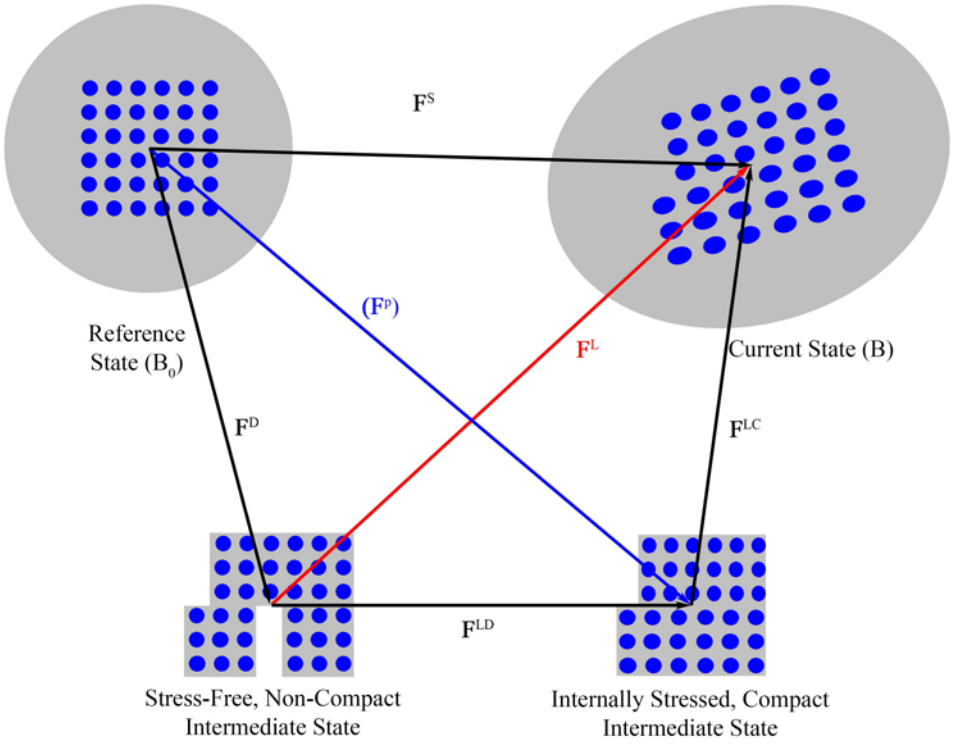

Figure 1. Deformation Mappings and Configurations for Single Crystal RVE

Finally, we note that in most crystal plasticity treatments "elastic" deformation corresponds to lattice deformation while "plastic" refers to permanent deformation caused by dislocation motion. In this work we choose to eschew the use of the terms elastic and plastic to refer to states of deformation that may contain incompatibility. We believe that this usage introduces widespread misunderstanding of the physical processes that create the deformed crystal. For example, when elastic deformation is defined as the deformation that is recovered when external loads are removed and plastic deformation as that which remains [11, 28] the plastic deformation so defined contains a component of lattice deformation due to the presence of internal defects. Since these terms are frequently employed in engineering applications of continuum plasticity to refer to deformation that does not specifically consider incompatibility of the crystal lattice, we prefer to avoid them in discussing crystal plasticity.

3.4 The Nye Tensor and Lattice Deformation

The local state of deformation of a crystal lattice is described in terms of the Nye tensor [27], lattice curvature tensor and the gradient of lattice strain [5]. The Burgers vector flux across an area element can be expressed in terms of either the True Burgers Vector (TBV), measured in the perfect reference lattice, or the Local Burgers Vector (LBV), measured in the deformed lattice. In this work we employ the TBV and the associated Nye tensor defined by Bilby:

$$\boldsymbol{\alpha} = -\nabla \times \mathbf{F}^{-L} \tag{21}$$

where the negative sign in the superscript indicates the inverse of the tensor. If all deformation components are small in the usual mathematical sense, the multiplicative decomposition of Equation (20) can be approximated by

$$\nabla \mathbf{u} \approx \boldsymbol{\beta}^{L} + \boldsymbol{\beta}^{D} \tag{22}$$

where $\boldsymbol{\beta}^{L}$ and $\boldsymbol{\beta}^{D}$ are, respectively, the distortion of the crystal lattice and the stress-free distortion due to dislocation motion. For this small deformation approximation $\mathbf{F}^{-L} \approx \mathbf{I} - \boldsymbol{\beta}^{L}$, leading to the relationship

$$\boldsymbol{\alpha} = \nabla \times \boldsymbol{\beta}^{L} \tag{23}$$

By Equation (22) and the continuity of **u**:

$$\boldsymbol{\alpha} = -\nabla \times \boldsymbol{\beta}^{D} \tag{24}$$

where the gradients in Equations (23) and (24) are taken in the appropriate coordinates.

While finite lattice deformations accompanied by gradients in lattice strain can occur in experiments such as bending of single crystal beams [26] and wedge indentation of single crystals [20], we observe that lattice strains and strain gradients are expected to be much smaller than lattice rotations and curvatures due to the fact that the former increase the internal energy density of the crystal while the latter do not. Thus the capacity of a crystalline material to sustain an increase in internal energy due to deformation does not impose limitations on lattice rotations and curvatures to the same extent that it does on lattice strains and strain gradients.

Employing the polar decomposition of $\mathbf{F}^{L}$ into a rotation matrix, $\mathbf{R}^{L}$ and a symmetric Cauchy-Green tensor, we observe that the dominant role of lattice rotation in lattice distortion permits replacing the Cauchy-Green tensor by **I,** the Identity Tensor. Then applying the definition of the Nye tensor, Equation (21), yields:

$$\boldsymbol{\alpha} = -\nabla \times \mathbf{R}^{-L} \tag{25}$$

Of the several possible methods of expressing $\mathbf{R}^{L}$ the Rodrigues rotation formula provides the most convenient form for this purpose [30]. In this description an arbitrary lattice vector is rotated in the right-handed sense through an angle θ about an axis parallel to the unit vector, **m**. The resulting rotation matrix is

$$\mathbf{R}^{L} = \mathbf{I}\cos\theta + \sin\theta\left[\mathbf{m}\right]_{\times} + \left(1-\cos\theta\right)\left(\mathbf{m}\otimes\mathbf{m}\right) \tag{26}$$

where the second-rank tensor operator $\left[\mathbf{m}\right]_{\times} = \mathbf{m}\times$. A more compact notation for subsequent operations can be developed in terms of the vector, $\boldsymbol{\varphi} = \mathbf{m}\sin\theta$, the dual vector to the rotation matrix. Utilizing the property of rotation matrices that the inverse is equal to the transpose and noting that the first and third terms of Equation (26) are symmetric permits us to write

$$\boldsymbol{\alpha} = \nabla \times \left[\boldsymbol{\varphi}\right]_{\times} \tag{27}$$

Then defining $\boldsymbol{\kappa} = \nabla\boldsymbol{\varphi}$, Equation (25) becomes

$$\boldsymbol{\alpha} = \mathbf{I}\left[\mathrm{Tr}\left(\boldsymbol{\kappa}\right)\right] - \tilde{\boldsymbol{\kappa}} \tag{28}$$

where the tilde indicates the transpose of the tensor and Tr(**X**) is the trace of **X**. Equation (28) is valid for both finite and infinitesimal deformation with the appropriate adjustments to the definition of $\boldsymbol{\varphi}$ for finite and infinitesimal lattice rotations.

3.4.1 Definition of the Dislocation Density Vector

In the following section we describe how the deformation of a crystal due to dislocation motion can be characterized by a set of vectors, lying in the active slip planes that characterize the dislocation content of each active slip system. The development begins by following the approach of Arsenlis and Parks [1] relating the Nye tensor and local lattice curvature to the Geometrically Necessary Dislocation (GND) density of a crystal [2]. However we depart from these authors in our choice of a measure of the dislocation density.

First, we note with A&P that the Nye tensor can be expressed in terms of a sum of dyadic products of vectors on each active slip system. One of these vectors is the Burgers vector, $\mathbf{b}^{(k)}$, on the k^{th} slip system and the other is related to the dislocation content and distribution on parallel slip planes of the k^{th} slip system that are contained in the volume element analyzed. These Dislocation Density Vectors (DDVs) and their associated Burgers vectors are related to the local state of lattice curvature and local gradients of lattice strain [13, 14].

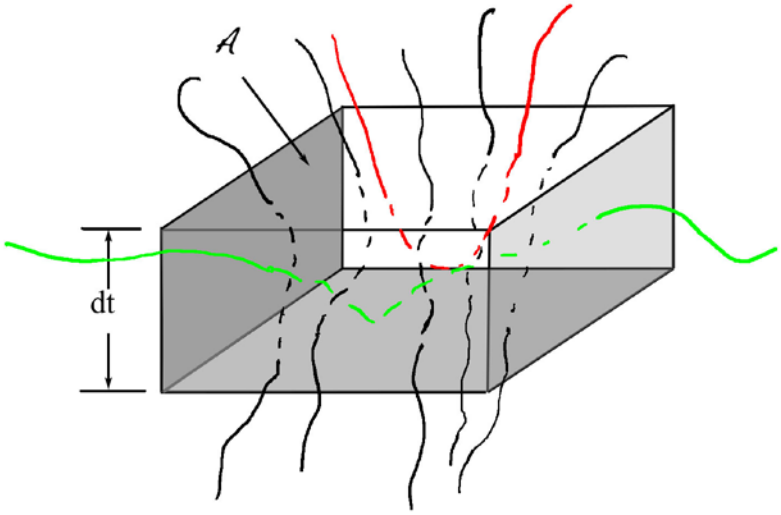

Figure 2. Dislocations Intersecting Volume Element

To determine the DDVs for each slip system we refer to Figure 2 illustrating a small volume element of thickness, dt, area, A, and unit normal, **n**. The volume element contains a distribution of dislocation lines that, for the sake of the present argument, all have the same Burgers vector, **b**. The parallel surfaces have unit outward normals, **n**, that are intersected by dislocations of various orientations. Some of these lines intersect parallel surfaces separated by dt, some intersect only one such surface and some lie on planes sufficiently near to being normal to **n** that they do not intersect the surfaces normal to **n** at all. In the subsequent discussion we consider only segments that intersect both surfaces normal to **n**.

As noted by Arsenlis and Parks, the contribution to lattice curvature due to a generally curved dislocation that intersects both surfaces normal to **n** is measured by the length connecting intersections on opposite surfaces. This is the component of length that contributes to the GND density. Any additional length due to the departure of the dislocation from a straight line contributes an equal length of dislocation line containing components of opposite sense that produce no net contribution to the local lattice curvature. This additional line length adds to the internal strain energy of the crystal, however, and constitutes the contribution of the dislocation segment to the Statistically Stored Dislocation (SSD) density [2].

With each dislocation segment contained in the volume element that intersects unit area normal to **n** we associate not only a Burgers vector, but also a unit tangent vector at the point of intersection with the surfaces normal to **n.** Choosing the Burgers vectors of all dislocations to have the same sense then requires us to assign a sense to each unit tangent vector, which we do following the FS/RH convention [4]. In this convention the sense vector of a r.h. screw dislocation is parallel to the Burgers vector, while a l.h. screw dislocation is anti-parallel to it, and the positive normal to the slip plane points towards the extra half-plane of a positive edge dislocation.

Considering the upper surface of the volume element, for which the outward pointing unit normal is +**n** , we note that the Burgers vector flux due to dislocations intersecting A is equal to the Burgers vector of a single dislocation times the *net* number of dislocations intersecting the area divided by the magnitude of A. The net number of dislocations intersecting A is determined by assigning a positive or negative value to each *intersection* according to whether the unit tangent vector of the dislocation, **t** , makes an acute (+) or obtuse (-) angle with **n** , corresponding to the dislocation entering or leaving the volume element. This condition can be expressed as $\text{sgn}\,[N^{(i)}] = \text{sgn}\,[\mathbf{n} \cdot \mathbf{t}^{(i)}]$, where $N^{(i)}$ refers to the intersection of the i^{th} dislocation with A and $\mathbf{t}^{(i)}$ is the unit tangent vector of the dislocation at the point of intersection. Using this convention for the sign of an intersection we define the total positive and negative intersections, N+ and N-, respectively. Clearly if these values are equal, the net Burgers vector flux vanishes for the area sampled.

Notice that this definition applies to the senses of *intersections with the sampling plane* not the *dislocations*. For a pair of dislocations to have opposite sense, each dislocation must have both its edge and screw components of opposite sense to the corresponding component of the other dislocation. Although no ambiguity can arise in assigning a positive or negative sense to pure edge or pure screw dislocations or to mixed dislocations in which both the edge and screw components are the same sense, it is not possible to devise a self-consistent convention for assigning a positive or negative sense to a general mixed dislocation. It is quite possible for two parallel mixed dislocations to have edge segments of the same sense and screw segments of opposite sense and vice versa. Thus is clearly inappropriate in such a case to assign a single sense to either dislocation. However no such ambiguity arises in assigning a sense to the intersection of dislocations with a sampling plane, as defined above.

Now consider a situation in which a single slip system is active, the senses of all intersections are the same and the total number of intersections is N. Referring to Figure 2 we note that the length, projected parallel to **n**, of each segment threading the volume element is equal to dt, regardless of the length of the segment itself. So the total *projected* length of dislocations piercing the element is equal to Ndt. The projected length per unit volume follows from dividing this length by the volume, V = A dt. This yields the result that $N_A(\mathbf{n})$, the number of

intersections per unit area normal to **n** , is equal to the length of dislocations, projected parallel to **n ,** per unit volume. We use this fact to define a DDV for each slip system, $\boldsymbol{\rho}^{(k)}$, such that $\boldsymbol{\rho}^{(k)} \cdot \mathbf{n} = N_A^{(k)}$ [13]. It follows that the dimensions of $\boldsymbol{\rho}^{(k)}$ are length per unit volume. Arsenlis and Parks employed a similar concept, but without defining a DDV related to the projected length of dislocations as described above.

3.4.2 Derived DDVs and Their Interpretation

In this section we develop further the concept of the DDV to illustrate how the concepts of the Geometrically Necessary Dislocation density, Statistically Stored Dislocation density and Total Dislocation Density can be related to the DDV definition[††]. This separation enables appropriate measures of dislocation content to be inserted in constitutive equations for the description of single crystal deformation. Finally we note that Dislocation Dynamics codes are all capable of providing output in the form of the Burgers vectors and the coordinates of the end points of dislocation segments at the end of each computation step. Thus numerical data for the computations outlined in the following discussion are readily available from such simulations.

Although the definition of the DDV described above is useful for relating the GND to the Nye tensor, the vector sum obscures some important aspects of the dislocation population. Additional information can be obtained by collecting screw and edge components of like sign to define signed components of the DDV. If only information on GND density is required, this separation into the sources of the edge and screw components is unnecessary. However consideration of the origins of the various components provides more useful detail on the character of the dislocation distribution.

In an earlier section we noted the impossibility of choosing a self-consistent definition of sign for a mixed dislocation. This proves problematical in relating the motion of actual dislocations to the DDV description, since the latter is based on the projected length of dislocations along the slip direction and Taylor axis. Accordingly, we propose a nomenclature for dislocations according to the relative signs of its edge and screw components. Using the FS/RH convention described earlier for relating the sense of the dislocation segment to the true Burgers vector, designate mixed dislocations whose edge and screw components have the *same* sense as Mixed Dislocations of the First Kind (1), and mixed dislocations whose edge and screw components have opposite senses, as Mixed Dislocations of the Second Kind (2). Pure edge and screw dislocation segments will be designated as the Zeroth Kind (0).

Using this naming convention the screw (S) and edge (E) components of the DDV due to dislocation segments of each kind, on a each slip system, become:

- S (E) components due to pure screw (edge) segments: $\boldsymbol{\rho}^{0}_{\pm S(E)}$
- S (E) components due to Mixed Dislocations of the First Kind: $\boldsymbol{\rho}^{1}_{\pm S(E)}$
- S (E) components due to Mixed Dislocations of the Second Kind: $\boldsymbol{\rho}^{2}_{\pm S(E)}$

[††] A portion of this work was performed while the author was a Visiting Researcher at MPIE, Düsseldorf, Germany.

The net projected length of screw and edge segments can now be expressed as

$$\rho_{S(E)} = \left(\sum_{N_{+S(E)}} \rho^{0}_{+S(E)} - \sum_{N_{-S(E)}} \rho^{0}_{-S(E)} \right) + \left(\sum_{N_{+1}} \rho^{1}_{+S(E)} - \sum_{N_{-1}} \rho^{1}_{-S(E)} \right) + \left(\sum_{N_{+2}} \rho^{2}_{+S(E)} - \sum_{N_{-2}} \rho^{2}_{-S(E)} \right) \tag{29}$$

where $N_{\pm i}$ are the numbers of the segments of the indicated type (i = 1,2,S,E) and sign. The magnitudes of the signed screw and edge components of the DDV can also be expressed in terms of this notation as follows:

$$\rho_{\pm S(E)} = \sum_{N_{\pm S(E)}} \rho^{0}_{\pm S(E)} + \sum_{N_{\pm 1}} \rho^{1}_{\pm S(E)} + \sum_{N_{\pm 2}} \rho^{2}_{\pm S(E)} \tag{30}$$

where the notation ±S(E) indicates that the expression applies to both screw (S) and edge (E) components with the indicated sign This procedure extends the definition of the DDV proposed by Hartley [12, 13, 14] consisting only of positive and negative components, ρ^{+} and ρ^{-}, which are formed by arbitrarily grouping projections of screw and edge segments having like sign without regard to the sense of the accompanying components. The screw component of ρ^{+} is ρ_{+S}, and the corresponding component of $\rho^{-}$is ρ_{-S}, with similar expressions relating the edge components.

Now we describe three derived vectors, ρ^{G}, ρ^{T} and ρ^{SS}, all formed from various combinations of the projected components described above. It should be noted, however, that only for ρ^{G} does the sense of the vector bear a direct physical significance to the resultant Burgers vector of the population. In fact the resultant Burgers vector of dislocations associated with ρ^{T} is the same as that for ρ^{G} and the resultant Burgers vector for ρ^{SS} vanishes by definition. The senses of ρ^{T} and ρ^{SS} are selected on the basis of consistency with the concept of conservation proposed by Ashby [2] for components of the scalar lengths per unit volume.

Dislocation segments in the population are projected parallel to η and ξ and summed to obtain the positive and negative screw and edge components as indicated by Equation (29) *et seq*. The sums of projections of the individual segments along $\pm\eta$ and $\pm\xi$ form the components $\rho_{\pm S(E)}$. Figure 3 shows a possible configuration.

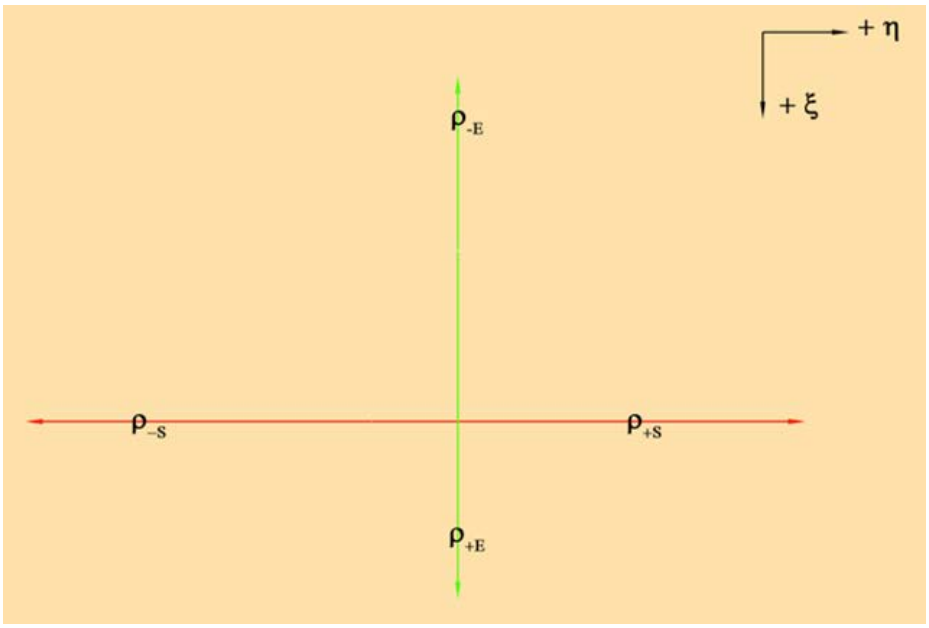

Figure 3. Possible Configuration of S and E Projections of DDV

As previously shown, the Geometrically Necessary DDV, ρ^G, is the residual DDV formed from the portion of the screw and edge segments that are unpaired with ones of like character and opposite sense. The edge and screw components of ρ^G can be expressed as:

$$\rho^G = \rho_S^G \eta + \rho_E^G \xi = \left(\rho_{+S} - \rho_{-S}\right)\eta + \left(\rho_{+E} - \rho_{-E}\right)\xi \tag{31}$$

This quantity is related to the *net* Burgers vector of the dislocation population. The relationship among the quantities is shown in Figure 4.

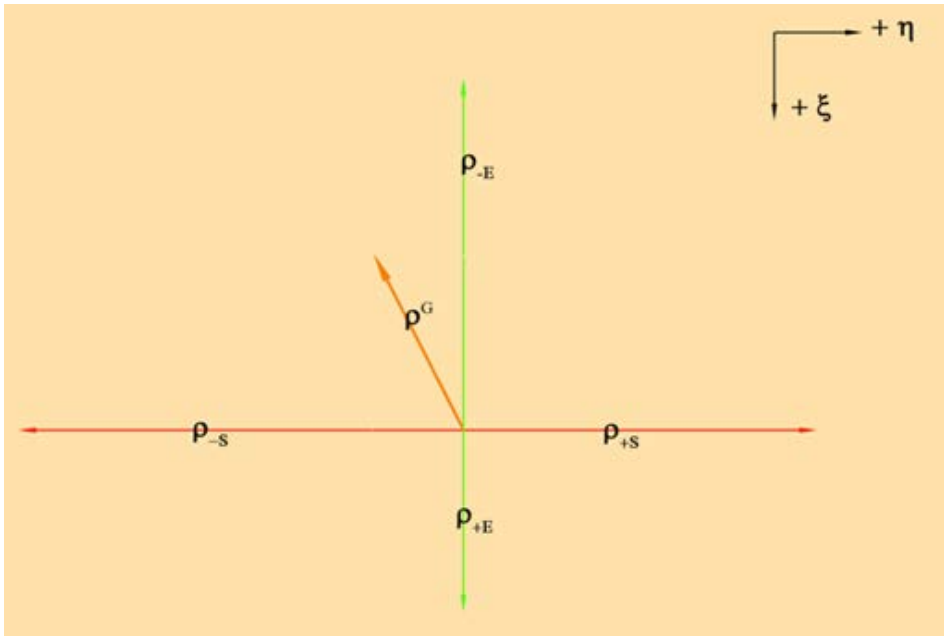

Figure 4. Relationship of GN DDV to S and E Components

In the example shown the numerically larger of both the screw and edge components of $\boldsymbol{\rho}^G$ are in the negative sense as shown by the direction of $\boldsymbol{\rho}^G$ in Figure 4.

A Total DDV, $\boldsymbol{\rho}^T$, can also be defined in terms of the total projected lengths of the screw and edge segments of the population. The magnitude of this vector is:

$$\left|\boldsymbol{\rho}^{\mathbf{T}}\right|^2 = \left|\boldsymbol{\rho}_{+\mathbf{S}} + \boldsymbol{\rho}_{-\mathbf{S}}\right|^2 + \left|\boldsymbol{\rho}_{+\mathbf{E}} + \boldsymbol{\rho}_{-\mathbf{E}}\right|^2 \tag{32}$$

while its direction is arbitrarily determined by requiring that it lie in the same quadrant as $\boldsymbol{\rho}^G$, i.e. $\boldsymbol{\rho}^T \cdot \boldsymbol{\rho}^G \geq 0$. Writing the Total DDV as

$$\boldsymbol{\rho}^{\mathbf{T}} = \left[2\mathrm{H}\left(\rho_{\mathrm{S}}^{\mathrm{G}}\right) - 1\right]\left(\boldsymbol{\rho}_{+\mathbf{S}} + \boldsymbol{\rho}_{-\mathbf{S}}\right)\eta + \left[2\mathrm{H}\left(\rho_{\mathrm{E}}^{\mathrm{G}}\right) - 1\right]\left(\boldsymbol{\rho}_{+\mathbf{E}} + \boldsymbol{\rho}_{-\mathbf{E}}\right)\xi \tag{33}$$

can satisfy this condition, where H(x) is the Heaviside Step function, H(x) = 1 when $x \geq 0$ and zero otherwise.

Since $\boldsymbol{\rho}^T$ is formed from the sums of projected segment lengths, its magnitude is not equal to the total length of dislocations per unit volume. However, if all dislocation segments are arcs of convex curves or closed convex curves lying in the same or parallel slip planes, the sum of the projected lengths along $\pm\eta$ and $\pm\xi$ (the L_1 norm of $\boldsymbol{\rho}^T$) forms an upper bound to the total length, while the magnitude of $\boldsymbol{\rho}^T$ (the L_2 norm) is a lower bound. Other dislocation arrangements that may lead to more complex relationships between the magnitude of the total DDV, the geometry of the actual dislocation array and the total dislocation line length will not be considered here.

While $\boldsymbol{\rho}^G$ is that part of the total DDV due to unpaired edge and screw segments, $\boldsymbol{\rho}^{SS}$, the Statistically Stored DDV, is formed from the projections of those segments of the population that have a counterpart of opposite sense. The quantities that represent the screw and edge components of a vector with the necessary property are the numerically smaller of the positive and negative components of the corresponding orientations. In the example given in Figure 3 it is evident that the positive screw and edge components are the smaller of the two values for each orientation. Consequently, for this example the magnitude of $\boldsymbol{\rho}^{SS}$ is equal to twice the magnitude of the resultant of these two components. The sense of $\boldsymbol{\rho}^{SS}$ follows from a conservation condition similar to that proposed by Ashby for the corresponding components of the scalar length per unit volume. In the spirit of Ashby's proposal, we define $\boldsymbol{\rho}^{SS}$ as the vector difference of $\boldsymbol{\rho}^T$ and $\boldsymbol{\rho}^G$, which can be written explicitly as the difference between Equations (39) and (37). Figure 5 corresponds to the physical situation represented in Figures 3 and 4.

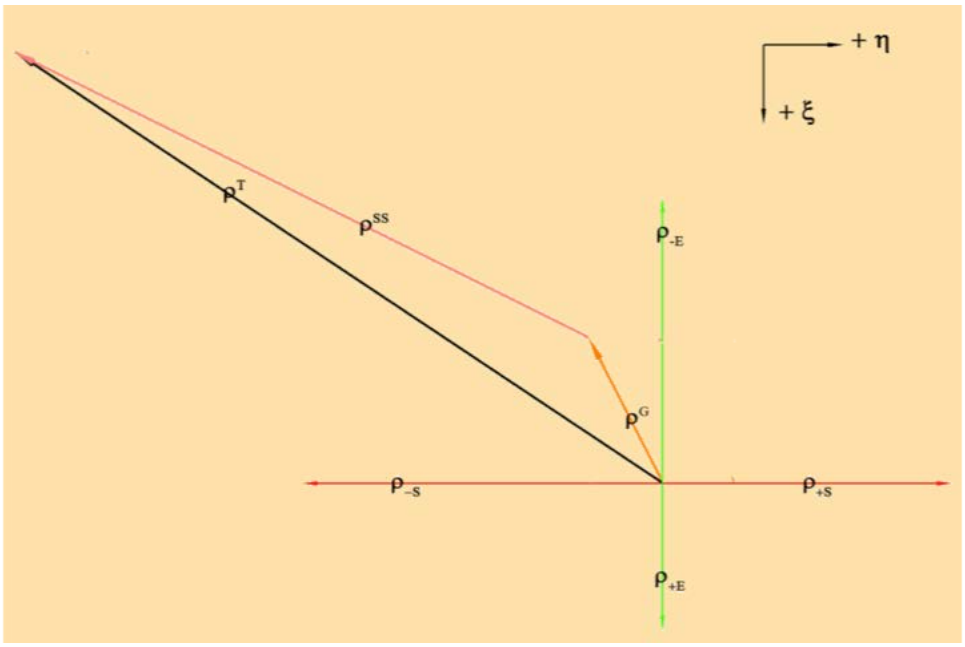

Figure 5. Relationship among Derived DDVs

The example in Figure 5. Relationship Among Derived DDVs must not be interpreted as meaning that the edge and screw components of $\boldsymbol{\rho}^{T}$ and $\boldsymbol{\rho}^{SS}$ have unique physical senses, since both vectors have contributions from both positive and negative edge and screw components of the dislocation distribution. Their sense is determined entirely by the conservation postulate, which requires that they lie in the same quadrant as $\boldsymbol{\rho}^{G}$, whose orientation does, however, have a unique physical significance. When the distribution of dislocations has a vanishing net Burgers vector, $\boldsymbol{\rho}^{G}$ is identically zero, $|\boldsymbol{\rho}^{T}| = |\boldsymbol{\rho}^{SS}|$ and the direction of the latter two derived vectors is indeterminate.

In a study of plane strain plasticity of a single crystal, Lardner proposed two tensors related to the Nye tensor [21]. One is associated with the "net" dislocation content and the other "total" dislocation content. The tensors are formed from two "signed" Nye tensors each defined as in Equation (31) but using dislocations of opposite signs. In this study the dislocation content was limited to two sets of edge dislocations with different Burgers vectors, so the non-uniqueness of the signs of dislocations does not arise as it does for the general case. Lardner's difference tensor, $\boldsymbol{\Delta}$, is the algebraic sum of these signed tensors, which yields the tensor originally derived by Nye. Lardner's Absolute tensor, $\boldsymbol{\Lambda}$, is the algebraic difference of these signed tensors for each active slip system. Although similar in form to the Nye tensor, this quantity does not bear a straightforward relationship to the changes in lattice geometry caused by dislocation motion. These concepts are difficult to generalize to a crystal deforming by mixed dislocations on multiple slip systems because of the uncertainty in assigning a unique sense to a general mixed dislocation, as described earlier.

The Nye tensor formed from a non-vanishing $\boldsymbol{\rho}^G$ does have a unique sense as shown in the definition. So $\boldsymbol{\Delta}$ is identical to $\boldsymbol{\rho}^G$. Since Lardner's definition for $\boldsymbol{\Lambda}$ is based on the difference of quantities of opposite sign, it includes contributions from all dislocation segments present, which logically associates it with $\boldsymbol{\rho}^T$:

$$\boldsymbol{\Lambda}=\mathbf{b} \times \boldsymbol{\rho}^T \tag{34}$$

It should be noted that the uniqueness of this definition depends on the existence of a non-vanishing $\boldsymbol{\rho}^G$, as discussed earlier. Although not included in Lardner's treatment, an additional tensor associated with $\boldsymbol{\rho}^{SS}$ can be similarly defined as

$$\boldsymbol{\Lambda}^S=\mathbf{b} \otimes \boldsymbol{\rho}^{SS} \tag{35}$$

The role of this tensor in Lardner's theory should be analogous to the role of $\boldsymbol{\rho}^{SS}$ in Ashby's description of the role of various components of the dislocation distribution in plastic deformation. The same caveat on uniqueness as for $\boldsymbol{\Lambda}$ applies to this tensor. As in the case of $\boldsymbol{\Lambda}$, this tensor is not related to changes in the lattice geometry.

3.5 Motion of Groups of Dislocations

The behavior of groups of dislocations is determined by their equilibrium positions under the action of external forces and mutual interaction forces under specified boundary conditions. This group response, an example of the phenomenon of *emergence* as defined for animated graphics simulations of flocking behavior, can be described by the behavior of moments of the distribution function for the group. Constitutive equations suitable for mesoscopic description of dislocation behavior can then be developed in terms of the response of these moments to the local stress environment expressed in terms of a virtual force on the configuration. Discrete DD simulations of dislocation configurations involve applying to elements of each dislocation in a computational cell the forces arising from interactions with other dislocations in the cell and lattice resistance forces under specified boundary conditions on the cell. A yet unexploited result from these computations is the capability for developing constitutive relations for the group behavior of dislocations at these scales. The goal of such an effort is to find appropriate relationships between the virtual force on the array and the resulting motion of the array. Before this can be accomplished, it is necessary to find methods of characterizing the dislocation array in terms of the properties of an appropriate distribution function.

The following discussion shows how centroids and dipole moments of the net distribution of dislocations can be measured. Arrays are then described in terms of dislocation density vectors for positive and negative dislocations located at the centroid of the respective arrays and motion of the arrays is described in terms of the motion of the centroids. The force on the arrays is the Peach-Koehler force on the dislocation density vectors. Stresses in the body outside the computational cell due to the dislocation array in the computational cell can be calculated in terms of the net dislocation density and the dipole strength of the array, taking the as origin the centroid of the computational cell.

As an example of such a calculation consider the following procedure for computing the dislocation density tensor, the centroids of the distributions and the dipole moments for a 2-dimensional array of dislocations. Consider an array of straight, mixed dislocations having zero net Burgers vector and lying on four slip systems in a body-centered cubic crystal. Let the unit tangent vectors parallel or antiparallel to $\left[0\,\bar{1}0\right]$. Two systems each are on (101) and

$(10\bar{1})$ planes, corresponding to the slip directions $[11\bar{1}]$ and $[1\bar{1}\bar{1}]$, and $[1\bar{1}1]$ and $[111]$, respectively. The sense of the Burgers vector of dislocations on each system is the same, with the sense of each dislocation given by the sense of its tangent vector. Horizontal and vertical axes are $[10\bar{1}]$ and $[101]$, respectively.

Applying the definition of the Nye tensor to dislocations on the $\pm k^{th}$ slip system gives

$$\alpha_{ij}^{(\pm k)} = n^{(\pm k)} b_i^{(k)} \xi_j^{(\pm k)} = b_i^{(k)} \rho_j^{(\pm k)} \tag{36}$$

where ± designates the sense of the quantity, $\xi^{(\pm k)}$ is a unit vector indicating the sense of the dislocation, $\mathbf{b}^{(k)}$ is the Burgers vector, $n^{(\pm k)}$ is the number of dislocations intersecting unit area normal to $\xi^{(\pm k)}$ and $\boldsymbol{\rho}^{(\pm k)} = n^{(\pm k)} \xi^{(\pm k)}$ is the dislocation density vector. Note that the sense of $\mathbf{b}$ is the same for both positive and negative values of ξ. Locations of dislocations in the computational cell are specified by their coordinates, $x_i^{(\pm k)}$, where i = 1,2. The centroid of each array is located at the average of coordinates for the type of dislocations in the array:

$$\bar{X}_i^{(\pm k)} = \left(\frac{1}{n^{(\pm k)}} \right) \sum_{m=1}^{n^{(\pm k)}} x_i^{(m)} \tag{37}$$

The velocity of each distribution, $\bar{V}_i^{(k)} = \dot{\bar{X}}_i^{(\pm k)}$, is defined as the time rate of change of its centroid. The dipole moment of the k^{th} array of positive and negative dislocations having the same Burgers vector but opposite sign is related to the separation of the centroids of their distributions:

$$\bar{D}_i^{(k)} = \bar{X}_i^{(+k)} - \bar{X}_i^{(-k)} = \left(\frac{1}{n^{(k)}} \right) \left[\sum_{m=1}^{n^{(k)}} x_i^{(+m)} - \sum_{m=1}^{n^{(k)}} x_i^{(-m)} \right] \tag{38}$$

since $n^{(+k)} = n^{(-k)} = n^{(k)}$. The dipole tensor per unit area for each slip system is

$$P_{ij}^{(k)} = n^{(k)} b_i^{(k)} \bar{D}_j^{(k)} \tag{39}$$

The force on each array is conveniently expressed in terms of a virtual (body) force on the dislocation density vector for each type of dislocation:

$$\tilde{f}_k^{(\pm k)} = \varepsilon_{krs} \sigma_{r\ell}^{(\pm k)} b_\ell^{(k)} \rho_s^{(\pm k)} \tag{40}$$

A mobility for each distribution can now be defined as the second rank tensor relating this force to the velocity of the configuration as defined above. These definitions permit a description of the results of DD simulations to be expressed in terms of continuum quantities that can be employed in the formulation of mesoscale constitutive laws for the behavior of dislocation arrays. Extension to 3D arrays is straightforward.

4.0 RESULTS AND DISCUSSION

4.1 Background

In experimental studies of the deformation of crystals, those that employ diffraction techniques using electrons, x-rays or neutrons provide information for the determination of lattice deformation. Present electron diffraction techniques now permit measurement of lattice rotations and strains over distances comparable to the spacing between dislocations. Complementary measurements of changes in the size and shape of grids applied to the surfaces or embedded within undeformed bodies give information for calculating shape deformation of the crystal. Combining these techniques offers an unprecedented opportunity for more detailed studies of the deformation of crystals at the micro-scale than has hitherto been possible.

Current advanced EBSD analyses of deformed single crystals are capable of detecting lattice rotations with a 3-micron spatial resolution [20]. This permits determination of local lattice curvatures and Nye tensor components from which lower bounds on the GND density can be computed. The distribution of GNDs on active slip planes can be further explored using concepts introduced by Arsenlis and Parks [1] and Hartley [12, 13]. In the following section we describe how plane strain deformation experiments of FCC crystals are employed to determine the character of the GND distribution, expressed in terms of the Dislocation Density Vector.

4.2 Plane Strain Deformation

Relationships among the amounts of dislocation motion on each slip system active in isochoric plane dislocation strain along the x_3 specimen axis follow from the conditions $\varepsilon^D_{i3} = \varepsilon^D_{3i} = 0$, and, since plane strain conditions require $\varepsilon^D_{33} = 0$, the constancy of volume leads to $\varepsilon^D_{11} + \varepsilon^D_{22} = 0$. Expressed in specimen coordinates dislocation (plastic) strain components in terms of dislocation motion on M slip systems become:

$$\varepsilon^D_{i3} + \varepsilon^D_{3i} = b\sum_{k=1}^{M} A^{(k)}\left[\eta_1^{(k)}\nu_3^{(k)} + \eta_3^{(k)}\nu_i^{(k)}\right] = 0\ , \quad i = 1\ldots3 \tag{41}$$

and

$$\varepsilon^D_{11} + \varepsilon^D_{22} = b\sum_{k=1}^{M} A^{(k)}\left[\eta_1^{(k)}\nu_1^{(k)} + \eta_2^{(k)}\nu_2^{(k)}\right] = 0 \tag{42}$$

where b is the magnitude of the Burgers vector (assumed to be equal on all active slip systems), $A^{(k)}$ is the magnitude of the area swept out by moving dislocations on the k^{th} slip system, and $\eta_i^{(k)}$ and $\nu_i^{(k)}$ are, respectively, components of unit vectors along the slip direction and normal to the slip plane of the k^{th} slip system, expressed in specimen coordinates. The terms in brackets in Equation (41) and (42) are components of the Schmid Tensors on the active slip systems. Each $A^{(k)}$ is the magnitude of a vector normal to the slip plane of the k^{th} slip system having a value equal to the net area swept out (per unit volume) by dislocations with Burgers vector $\mathbf{b}^{(k)}$ during the deformation process.

Equation (41) and (42) show that there are four independent as s for the twelve $A^{(k)}$. Since this is generally fewer than the unknown $A^{(k)}$, a lower bound for the $A^{(k)}$ can be obtained by solving Equation (41) and (42) using the Simplex method with the constraint that the sum of the absolute

values of the $A^{(k)}$ be a minimum, similar to the procedure by which a lower bound to the GN DDV components is obtained from measurements of the Nye tensor [1].

Since each slip plane in FCC crystals has three possible slip systems, a strain component due to slip on a particular plane is not uniquely associated with slip by dislocations of a particular Burgers vector. Slip system coordinates must be selected so that the sum of Burgers vectors that share a common slip plane sum to zero. Then a negative value for $A^{(k)}$ indicates dislocation motion on that slip plane in a sense opposite to that assumed. An estimate of the relative values of the resolved shear stresses on the slip systems follows from constructing an effective "plane strain stress tensor" that can be used to determine which slip systems have a vanishing resolved shear stress [20].

The local state of deformation of a crystal lattice is described in terms of the second rank Nye tensor, α, the gradient of lattice strain and the lattice curvature tensor, $\kappa = \nabla\varphi$, where φ is the dual vector of the lattice rotation tensor, $\mathbf{R}^{L}$. For situations where lattice strains and strain gradients are negligible relative to lattice rotations

$$\alpha = \mathbf{I}[\mathrm{Tr}(\kappa)] - \tilde{\kappa} \tag{43}$$

where **I** is the unit tensor, Tr(**X**) is the trace of **X** and the tilde indicates the transpose. When finite lattice deformations occur in experiments such as bending of single crystal beams [25] and wedge indentation of single crystals we expect these conditions to be satisfied.

4.3 Nye Tensor Components

Finally we note that the Nye tensor can be expressed in terms of a sum of dyadic products of vectors on each active slip system. One of these vectors is the Burgers vector, $\mathbf{b}^{(k)}$, on the k^{th} slip system and the other is related to the dislocation content and distribution on parallel slip planes of the k^{th} slip system that are contained in the volume element analyzed. These DDVs and their associated Burgers vectors are related to the local Nye tensor components for the k^{th} slip system.

The Nye tensor relates the Burgers vector flux, **B,** across a plane to the orientation of the plane. For M active slip systems

$$\mathbf{B} = \sum_{k=1}^{M} \mathbf{b}^{(k)} N_{A}^{(k)} = \alpha \cdot \mathbf{n} \tag{44}$$

Replacing $N_{A}^{(k)}$ by its definition above gives

$$\sum_{k=1}^{M} \mathbf{b}^{(k)} \left[\rho^{(k)} \cdot \mathbf{n} \right] = \alpha \cdot \mathbf{n} \tag{45}$$

whence we obtain the relationship

$$\alpha = \sum_{k=1}^{M} \alpha^{(k)} = \sum_{k=1}^{M} \left[\mathbf{b}^{(k)} \otimes \rho^{(k)} \right] \tag{46}$$

in terms of Nye tensors and DDVs for each active slip system. Then according to Equation (46) the Nye tensor for each slip system is the dyadic product of the Burgers vector and the DDV for that system.

On each slip system the DDV can be expressed in terms of a component parallel to the slip direction, $\rho_S^{(k)}$, and a component normal to the slip direction, $\rho_E^{(k)}$. The angle Ψ, defined by

$$\Psi = \tan^{-1}\left[\rho_E^{(k)} / \rho_S^{(k)}\right] \tag{47}$$

is a measure of the screw-edge character of the GND distribution on the k^{th} slip system. The trace of the Nye tensor, $\mathrm{Tr}(\alpha)$, is

$$\mathrm{Tr}(\alpha) = \sum_{k=1}^{M} \mathbf{b}^{(k)} \cdot \rho^{(k)} = b\sum_{k=1}^{M} \rho_S^{(k)} \tag{48}$$

which clearly depends only on the screw components of the DDV on each slip system. Also, the vector product of the Burgers vector and the DDV on each system is a vector normal to the slip plane of the system. So the dual vector associated with the Nye tensor,

$$\vec{\alpha} = b\sum_{k=1}^{M}\left[\eta^{(k)} \times \rho^{(k)}\right] = b\sum_{k=1}^{M} \upsilon^{(k)}\rho_E^{(k)} \tag{49}$$

depends only on the edge components of the DDVs. It is the sum of vectors normal to each slip plane, each having a magnitude equal to the product of the Burgers vector and the edge component of the DDV on each slip system.

5.0 CONCLUSIONS AND RECOMMENDATIONS

Research performed on this subcontract has provided the theoretical and analytical foundation for the treatment of data obtained by Dislocation Dynamics simulations and experimental studies of single crystal deformation to provide constitutive relations relating the local state of stress to the content and motion of dislocation populations.

6.0 REFERENCES

[1] Arsenlis, A., & Parks, D. M. (1999). Crystallographic Aspects of Geometrically-Necessary and Statistically-Stored Dislocation Density. *Acta Materilia , 47*, 1597-1611.

[2] Ashby, M. F. (1970). The Deformation of Plastically Non-homogeneous Materials. *Philosophical Magazine , 21*, 399-424.

[3] Beaudoin, A. J., Mathur, K. K., Dawson, P. R., & Johnson, C. C. (1993). Three-dimensional deformation process simulation with explicit use of polycrystal plasticity models. *International Journal of Plasticity , 9* (7), 833-860.

[4] Bilby, B. A., Bullough, R., & Smith, E. (1955). Continuous distributions of dislocations: a new application of the methods of non-Riemannian geometry. *Proceedings of the Royal Society of London , A231*, 263-273.

[5] Bilby, B. A., Gardner, L. T., & Smith, E. (1958). The Relationship Between Dislocation Density and Stress. *Acta Metallurgica , 6* (1), 29-33.

[6] Clayton, J. D., & McDowell, D. L. (2003). A multiscale multiplicative decomposition for elastoplasticity of polycrystals. *International Journal of Plasticity , 19* (9), 1401-1444.

[7] Eshelby, J. D. (1957). The determination of the elastic field of an ellipsoidal inclusion and related problems. *Proceedings of the Royal Society of London, Series A , A241*, 376 - 396.

[8] Fleck, N. A., Muller, G. M., Ashby, M. F., & Hutchinson, J. W. (1994). Strain gradient plasticity: theory and experiment. *Acta Metallurgica et Materialia , 42* (2), 475-487.

[9] Gerken, J. M., & Dawson, P. R. (2008). A crystal plasticity model that incorporates stresses and strains due to slip gradients. *Journal of the Mechanics and Physics of Solids, 56* (4), 1651-1672.

[10] Gullett, P. M., Horstmeyer, M. F., Baskes, M. I., & Fang, H. (2008). A deformation gradient tensor and strain tensors for atomistic simulations. *Modelling Simul. Mater. Sci. Eng., 16* (1), 1-17.

[11] Gurtin, M. E. (2010). A finite-deformation, gradient theory of single-crystal plasticity with free energy dependent on the accumulation of geometrically necessary dislocations. *International Journal of Plasticity , 26* (8), 1073-1096.

[12] Hartley, C. S. (2003). A method for linking thermally activated dislocation mechanisms of yielding with continuum plasticity theory. *Philosophical Magazine , 83* (31-34), 3783-3808.

[13] Hartley, C. S. (2001). Multi-scale modeling of dislocation processes. *Materials Science and Engineering A , 319-321*, 133-138.

[14] Hartley, C. S. (2004). Representation of Dislocation Content by a Dislocation Density Vector. In N. M. Ghoniem (Ed.), *Proceedings of MMM 2* (pp. 59-61). Los Angeles, CA: Department of Mecanical and Aerospace Engineering, UCLA.

[15] Hartley, C. S., & Mishin, Y. (2005). Characterization and visualization of the lattice misfit associated with dislocation cores. *Acta Materialia , 53*, 1313-1321.

[16] Henann, D. L., & Anand, L. (2009). A large deformation theory for rate-dependent elastic--plastic materials with combined isotropic and kinematic hardening. *International Journal of Plasticity , 25* (10), 1833-1878.

[17] Kröner, E. (1960). Allgemeine Kontinuumstheorie der Versetzungen und Eigenspannungen. *Arch. Rational Mech. Anal. , 274-334*, 18-.

[18] Kröner, E. (1980). Continuum Theory of Defects. In R. Balian, M. Kleman, & J.-P. Poirier (Ed.), *Les Houches Summer School Session XXXV* (pp. 219-315). Amsterdam, NL: North-Holland Publishing Company.

[19] Kröner, E. (1958). *Kontinuumstheorie der versetzungen und eigenspannungen* (Vol. 5). Berlin: Springer Verlag.

[20] Kysar, J. W., Saito, Y., Oztop, M. S., Lee, D., & Huh, W. T. (2010). Experimental lower bounds on geometrically necessary dislocation density. (A. Khan, Ed.) *International Journal of Plasticity , 26*, 1097-1123.

[21] Lardner, R. W. (1969). Plane Strain Plasticity of Single Crystals. *International Journal of Engineering Science , 7*, 417-425.

[22] Lee, E. H., & Liu, D. T. (1967). Elastic-Plastic Theory with Application to Plane-Wave Analysis. *Journal of Applied Physics , 38* (1), 19-27.

[23] Lion, A. (2000). Constitutive modelling in finite thermoviscoplasticity: a physical approach based on nonlinear rheological models. *International Journal of Plasticity , 16* (5), 469-494.

[24] McDowell, D. L. (2008). Viscoplasticity of heterogeneous metallic materials. *Materials Science and Engineering R , R 62*, 67-123.

[25] Motz, C., & Dunstan, D. J. (2012). Observation of the critical thickness phenomenom in dislocation dynamics simulation of microbeam bending. *Acta Materialia , 60*, 1603-1609.

[26] Motz, C., Weygand, D., Senger, J., & Gumbsch, P. (2008). Micro-bending tests: A comparison between three-dimensional discrete dislocation dynamics simulations and experiments. *Acta Materialia , 56* (9), 1942-1955.

[27] Nye, J. F. (1953). Some Geometrical Relations in Dislocated Crystals. *Acta Metallurgica , 1*, 153-162.

[28] Roters, F., Eisenlohr, P., Hantcherli, L., Tjahjanto, D. D., Bieler, T. R., & Raabe, D. (2010). Overview of constitutive laws, kinematics, homogenization and multiscale methods in crystal plasticity finite-element modeling: Theory, experiments, applications. *Acta Materialia , 58* (4), 1152-1211.

[29] Stukowski, A., & Arsenlis, A. (2012). On the elastic--plastic decomposition of crystal deformation at the atomic scale. *Modelling and Simulation in Materials Science and Engineering , 20* (3), 035012.

[30] Sun, S., Adams, B. L., & King, W. L. (2000). Observations of lattice curvature near the interface of a deformed aluminium bicrystal. *Philosophical Magazine A , 80* (1), 9-25.

[31] Teodosiu, C. (1970). A Dynamic Theory of Dislocations and its Application to the Elastic-Plastic Continuum. In J. A. Simmons, R. Bullough, & R. DeWit (Ed.), *Fundamental Aspects of Dislocaton Theory. II*, pp. 837-876. Gaithersburg: National Bureau of Standards.

[32] Teodosiu, C., & Sidoroff, F. (1976). A theory of finite elastoviscoplasticity of single crystals. *International Journal of Engineering Science , 14* (2), 165-176.

[33] Uchic, M. D., Dimiduk, D. M., Florando, J. N., & Nix, W. D. (2004). Sample dimensions influence strength and crystal plasticity. *Science , 305* (5686), 986-989.

[34] Uchic, M. D., Shade, P. A., & Dimiduk, D. M. (2009). Plasticity of micrometer-scale single crystals in compression. *Annual Review of Materials Research , 39*, 361-386.

LIST OF SYMBOLS, ABBREVIATIONS, AND ACRONYMS

AFM	Atomic Force Microscopy
AFRL	Air Force Research Laboratory
CR&D III	Collaborative Research and Development III
DD	Dislocation Dynamics
DDVs	Dislocation Density Vectors
DOD	Department of Defense
DTIC	Defense Technical Information Center
EAR	Export Administration Regulation
GND	Geometrically Necessary Dislocation
ITAR	International Traffic in Arms Regulation
LBV	Local Burgers Vector
MCE	Micro-Constitutive Equations
R&D	Research and Development
RVE	Representative Volume Element
RX	Materials and Manufacturing Directorate
RXC	Structural Materials Division
RXCM	Metals Branch
SSD	Statistically Stored Dislocation
SVE	Statistical Volume Element
TBV	True Burgers Vector
USAF	United States Air Force
WPAFB	Wright-Patterson Air Force Base